International Journal of Technology 14(4) 823-832 (2023)
Received August 2022 / Revised October 2022 / Accepted January 2023

International Journal of Technology

http://ijtech.eng.ui.ac.id

The Evaluation of Displacement Ductility of Low Confinement Spun Pile to Pile Cap Connections

Mulia Orientilize[1*], Widjojo A Prakoso[1], Yuskar Lase[1], Sidiq Purnomo[2], Ignatius Harry Sumartono[2], Winda Agustin[2]

[1]*Civil Engineering Department, Faculty of Engineering, Universitas Indonesia, Kampus UI Depok, 16424, Indonesia*
[2]*PT Wijaya Karya Beton Tbk, WIKA Tower 1 FL. 2-5, Jl. D.I. Panjaitan Kav. 9-10 Jakarta, 13340, Indonesia*

Abstract. Experimental study was carried out on three low confinement spun piles to pile cap connections. The detail followed the typically fixed connection in Indonesia. Reinforced concrete was filled to the spun pile to strengthen the connection region, except SPPC01. Different concrete types were used, shrinkage and non-shrinkage for SPPC02 and SPPC03, respectively. SPPC02 and SPPC03 could reach the targeted drift of 3.5% whereas SPPC01 was stopped at a drift of 2.75%. There was no shear failure detected during the test. The connection behaved as a fixed connection indicated by the fracture failure of the prestressed bars near the connection region. Analysis of the test results focused on displacement ductility. Two definitions of yield and ultimate displacement were employed to seek the possible ductility values. It varied from 3.05 to 6.04 for SPPC01 and from 3.01 to 4.95 for SPPC02 and SPPC03. The non-shrinkage concrete did not affect the strength of the connection but slightly improved the post-peak behavior. The ductility is 6–12% higher than spun piles with ordinary concrete. According to the limited ductility referring to ATC 96, JRA 2002, and AASHTO 2011, all specimens could achieve target ductility 3. Hence, it can be concluded that the low confinement spun pile connections performed well in displacement ductility.

Keywords: Displacement ductility; Experimental study; Low-confinement; Spun pile

1. Introduction

The connection of pile to pile cap in the foundation plays an important role to transfer the force from the upper to the bottom structure and vice versa. This part is critical since the change of area, stress, and stiffness occurs suddenly (Bang *et al.*, 2016). It needs rigorous detail and, usually, it is designed as a rigid connection that induces maximum curvature. Designing this part as a linear structure during a severe earthquake is costly. Currently, the design concept of the foundation has been moved forward to performance-based design (PBD). The pile is allowed to behave beyond its elastic stage to absorb the earthquake energy. Sufficient strength and ductility are essential to survive during a severe earthquake. Several countries have implemented PBD although the research is still carried out as indicated by international journal articles until 2021. Ductility is one of the important parameters to describe the seismic performance of a structure. It defines the ability of a structure to experience large amplitude cyclic deformation in the inelastic range without a

*Corresponding author's email: mulia@eng.ai.ac.is, Tel.: +62-21-7270029
doi: 10.14716/ijtech.v14i4.5889

substantial reduction in strength (Ling *et al.*, 2023).

NEHRP (FEMA P-750, 2009) classifies ductility demand according to the seismic zone. High seismic risk requires a ductility capacity of more than eight and the moderate seismic risk category requires more than four. According to Article C4.7.1 (AASHTO, 2011) for the life safety performance level, inelastic deformation in the piles is permitted but it should be limited to prevent severe damage. Hence, four is the maximum ductility suggested for the foundation. ATC 96 and JRA 2002 limit the ductility to three and the damage is allowed near the ground surface for accessible repair. Similar regulation is also adopted in the New Zealand code for highway bridges, where design ductility is limited to four for plastic hinges expected at a depth less than two meters below the ground level. For deeper plastic hinges, it should be limited to three (Chai and Hutchinson, 2002).

Several methods have been proposed to estimate the displacement ductility of the pile. Curvature ductility is one of the main factors affecting it. To be ductile, the pile section should meet the required curvature ductility demand (Budek-Schmeisser and Benzoni, 2008). A simplification approach to determine the displacement ductility of a pile embedded in single-layer soil was conducted by (Chiou *et al.*, 2011). Three parameters affect the values, which are curvature ductility (CD), overstrength ratio (OSR), and pile-soil interaction. Curvature ductility contributes the most, followed by the overstrength ratio. The moment-curvature is assumed as bilinear and the ductility is determined as the ratio of peak to the yield displacement. If the pile is in non-cohesive soil, estimation of the ductility is purely based on CD and OSR, while soil structure interaction affects the pile in cohesive soil. Although the equation could determine the ductility accurately only in cohesive soil, in general, the equation can be used to predict the ductility capacity of the pile.

The spun pile is a precast prestressed pile that is massively used in bridges and wharves. Experimental and numerical studies of this pile and its connection to the pile cap have been performed by many researchers. In China, the study was performed on different connection details (Wang *et al.*, 2014; Yang and Wang, 2016). There were six specimens tested with lateral cyclic loading and axial load. All of the specimens showed flexural damage. The study found that the ductility of the connection was in the range of 2.5 to 3.00. The study conducted by (Guo *et al.*, 2017) improved the ductility of the connection by adding two different strengthening to the connection area. The ductility increased from 3.07 to 4.31 and 5.48.

(Bang *et al.*, 2016) conducted testing of spun pile connection with no axial load. The pile was strengthened with different reinforcements, a deformed bar (PHC-B), and more shear reinforcement (PHC-C). Better energy absorption and ductility were observed on PHC-C where the value was 4.15 meanwhile PHC-B had a ductility of 2.75. A recent study on improved spun pile connection was conducted by Yang, Li, and Nan (2020). Four specimens with different improvements were tested until failure. Overall, the ductility of all specimens was in the range of 2.42 to 3.52.

In Indonesia, the spun pile is produced with a limited amount of transverse reinforcement and below the minimum requirement in accordance with (ACI Committe, 2019). This is because Indonesia still adopts the elastic concept where ductile performance is considered not necessary. Inconsistently, the code requires sufficient transverse reinforcement. It is known that the appropriate confinement is necessary to gain ductile performance. An experimental study of low confinement of the spun pile in Indonesia has been conducted by (Irawan *et al.*, 2018). The amount of transverse reinforcement was 0.24% which is about 21% of the minimum requirement. The study found that the confinement was insufficient to resist the explosion of the pile's concrete at the ultimate

state due to compression. The ductility of the spun piles was 2.50 and 4.50. Since the value was below 5, the study concluded that the piles were only suitable for low seismic-risk regions (Irawan *et al.*, 2017) ono. onoA onostudy of insufficient confinement of spun piles was also reported by (Budek and Benzoni, 2009) slightly below the minimum requirement of ACI 318-05 which was 1.2%. The research reported that the pile performed ductile where the ductility was two.

Indonesia should move forward to PBD for the bottom structure since based on the recent seismic risk map, where the ground acceleration tends to increase (Pramono *et al.*, 2020). Hence, the structural component should have adequate ductility. The spun pile with limited transverse reinforcement needs an assessment. The study aimed to obtain the performance of the spun pile to pile cap connection based on the common practice in Indonesia. The results could provide insight into the implementation of PBD in Indonesia. The evaluation was focused on displacement ductility based on the experimental result. Several values of ductility from different methods were presented to get a comprehensive result. Thus, the adequacy of the piles under severe seismic can be clarified.

2. Methods

Three full-scale spun pile connections were tested until failure to evaluate their seismic performance. To represent the real condition, the pile was picked from the stocking yard. A length of 220mm was cut from the middle part which has less confinement according to the research objective. The spiral pitch is 120mm where the volumetric ratio is 0,113%. To clarify the quantity of transverse reinforcement, the amount is compared to three equations and presented in Table 1. As can be seen, the equations result in different required quantities. The revised equation proposed by (Fanous *et al.*, 2010) results in higher minimum reinforcement. The required confinement of the spun pile used in this study cannot be determined since the equation proposed is only for piles with curvature ductility capacity greater than 18. Based on these equations, the spun pile employed in this study had less than 15% of the minimum requirements.

Table 1 The requirement of transverse reinforcement

Design Code	Requirement Transverse Reinforcement	The Minimum Values
SNI 1726:2012 article 7.14.2.2.5 refer to ASCE 7-16	$\rho_{=}0.25\frac{f_{c'}}{f_{yh}}\left(\frac{A_g}{A_{ch}}-1\right)\left(0.5+\frac{1.4P}{A_g f_{c'}}\right)=2.18\%$	$\rho_{min_{=}}0.12\frac{f_{c'}}{f_{yh}}\left(0.5+\frac{1.4P}{A_g f_{c'}}\right)=0.84\%$
SNI 2847-19 article 25.7.3.3 refer to ACI 318-19	$\rho_{=}0.45\left(\frac{A_g}{A_{ch}}-1\right)\frac{f_{c'}}{f_{yt}}=6.13\%$	$\rho_{min=}0.12\frac{f_{c'}}{f_{yh}}=1.31\%$
Revised equation (Fanous *et al.*, 2010) :	$\rho_{=}0.06\left(\frac{f_{c'}}{f_{yh}}\right)\left(\frac{\mu_o}{18}\right)\left(2.8+\frac{1.25P}{0.53f_{c'}A_{ch}}\right)=NA$	$\rho_{min=}0.168\frac{f_{c'}}{f_{yh}}=1.84\%$

2.1. The Specimens

Figure 1 shows the DED of the specimens. The 450mm in diameter spun pile was chosen with a wall thickness of 80mm. The spun pile was made of 57Mpa of concrete strength, reinforced by a 10@7.1mm PC bar, and confined by a spiral of 4mm in diameter. The connection between the spun pile and the pile cap was designed based on the common practice in Indonesia. The spun pile was embedded in the pile cap at a depth of 100mm. The required embedment length of the rebar was 620mm. To reduce the depth of the pile cap, the length was 500mm straight and the 200mm was bent 30 degrees as shown in Figure 1.

SPPC01 was an empty spun pile, whereas SPPC02 and SPPC03 were filled with concrete and reinforced by 6D19 as shown in Figure 2.

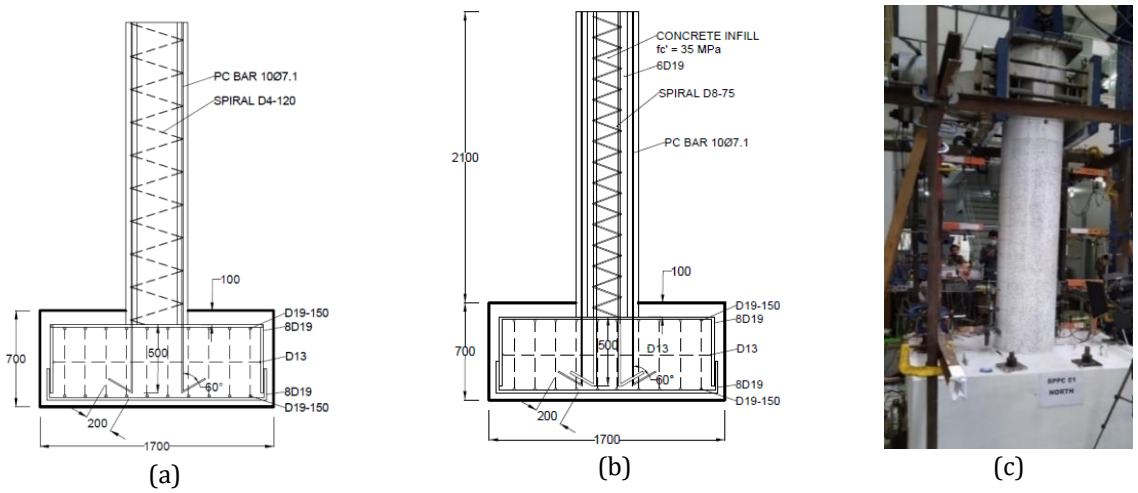

Figure 1 The connection details (a) SPPC01; (b) SPPC02/3 and (c) the test set-up

SPPC02 represents the typical connection where for ease in construction the concrete infill was cast together with the pile cap. Additional rebar of 6D19 was added and embedded into the pile cap to improve the connection strength. Shrinkage of the concrete infill was a concern and therefore in the preceding research, non-shrink concrete was used (Guo *et al.*, 2017; Bang *et al.*, 2016; Yang and Wang, 2016; Wang *et al.*, 2014). In this research, SPPC03 was filled with non-shrink concrete with *fc'* as 54.3MPa to see the effect of the concrete type on the behavior of spun pile connection.

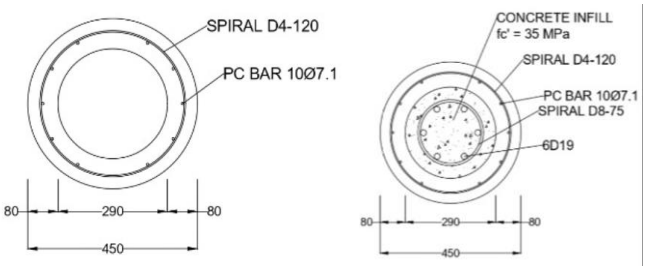

Table 2 The Steel Strength

Steel	*fy* (Mpa)	*fu* (Mpa)
Prestress (f7.1)	1274	1440
Stirrup (d4)	390	703
Rebar (D19)	400	570
Stirrup (d8)	240	370

Figure 2 The cross-section of SPPC01 and SPPC02

The pile cap was cast by 30Mpa of concrete strength and the actual strength of 28 days age was 34MPa. Due to the pandemic situation, the experimental test was delayed and the concrete age of SPPC03 was based on a 56-day test which was 36.5 MPa. The strength of steel employed in the experiment is presented in Table 1.

2.2. The Test Set-Up

Figure 1 shows the test setup. The specimen was attached to a strong floor and tied with 10 anchoring bolts. It was loaded vertically as 500kN which was equal to 0.1fc'Ag. A reverse cyclic lateral load was applied after the vertical force was fully applied. The horizontal loading protocol followed the ACI 437-07, where the test was conducted until a targeted drift of 3.5% was achieved or until the strength of the specimen was dropped by more than 25%. Seven and two transducers were employed to measure horizontal and vertical displacement, respectively. The concrete strain gauge was put on the spun pile and pile cap which was located 100mm from the connection. The strain of the reinforcement bar was measured through 6 strain gauges which were placed next to the connection in the loading plane. Meanwhile, four strain gauges were attached to the prestressed wire at a similar location.

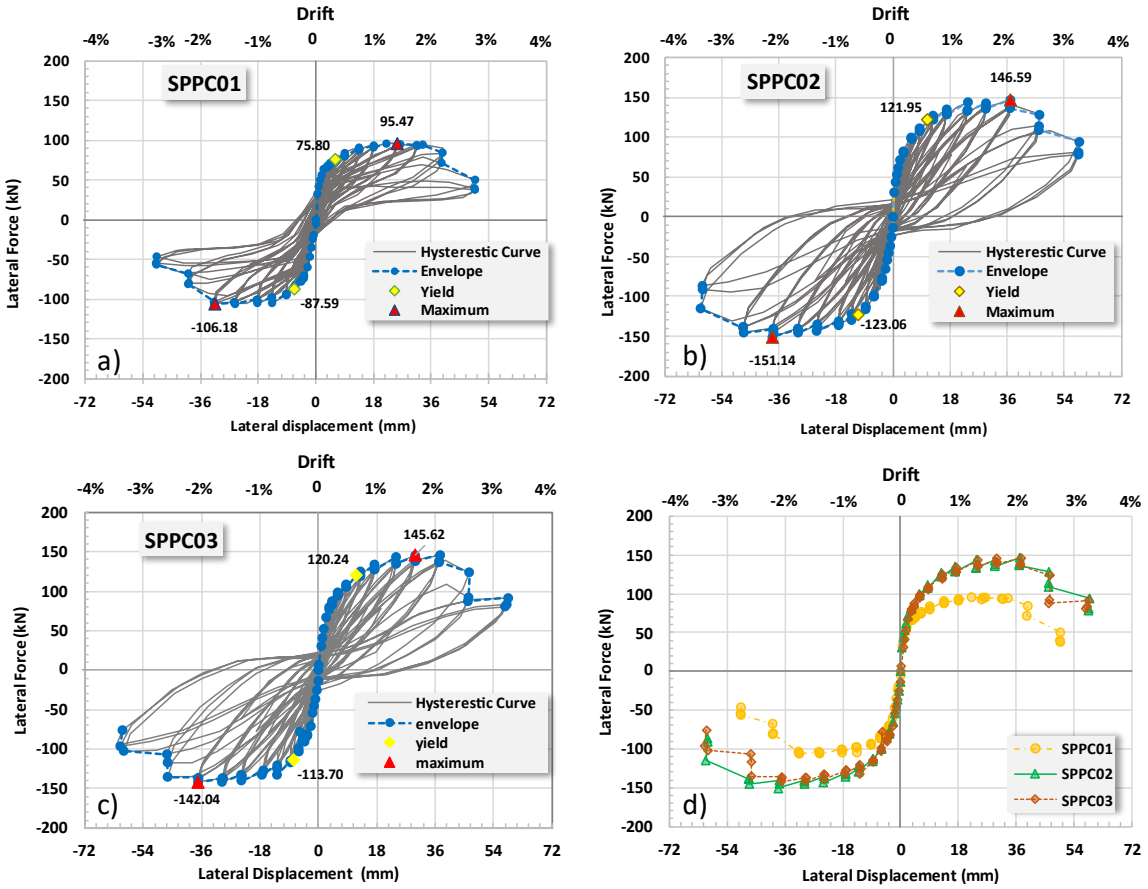

Figure 3 The hysteretic curves a) SPPC01; (b) SPPC02, (c) SPPC03, (d) Comparison of the envelopes curves

3. Results and Discussion

3.1. The Hysteretic Curves

SPPC02 and SPPC03 were tested until they reached a drift of 3.5% whereas SPPC01 was stopped at a drift of 2.75% since its strength drop more than 50%. Figure 3 shows the hysteretic curve and the envelope of all specimens. As can be seen, the presence of the reinforced concrete infill in SPPC02 and SPPC03 changes the performance of the spun pile connection significantly. It improves strength and energy absorption. The envelope of SPPC02 and SPPC03 are very closed which indicates that different concrete type does not affect the strength of the connection.

3.2. The Crack Pattern

The crack pattern on the spun pile is shown in Figure 4. There was a slight shear-flexural crack was detected at several places. The crack initiated from the tensile face and propagated to the center of the spun pile. The majority of the crack was a result of flexural failure. The crack propagated until 650mm from the connection region of SPPC02 and almost 800mm of SPPC03. Meanwhile, the last crack of SPPC01 was detected at depth of 400mm above the connection.

Light damage was found on the pile cap of SPPC01. Concrete crushing of the pile at the connection region was observed when drift reach 2%. A similar failure mode occurred on SPPC02 and SPPC03. The first crack of the spun pile was at a drift of 0.35% and 0.5%. The pile cap suffered moderate damage where a crack was detected on its surface with a depth

of less than 100mm. It started from the connection region and then it propagated to a radius of 150 to 180mm from the pile face.

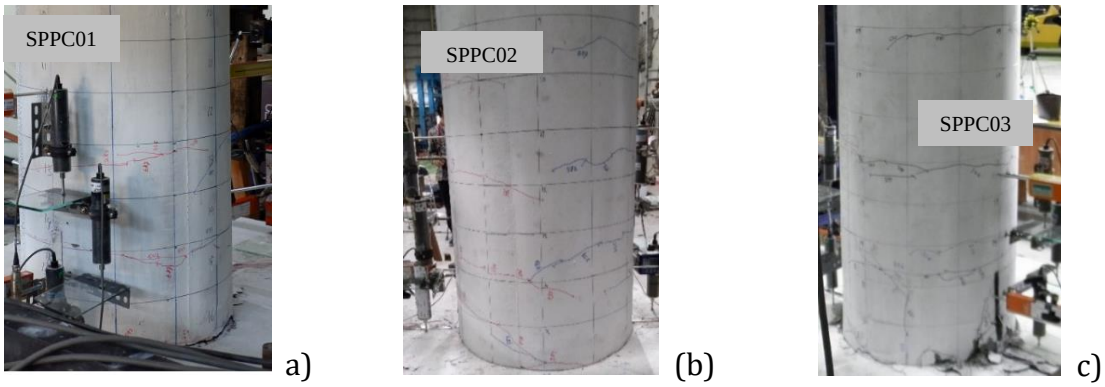

Figure 4 The Crack Patterns (a)SPPC01, (b) SPPC02, (c) SPPC03

The prestressed wires of all specimens suffered a fracture. Nine bars of SPPC01 were found fractured and one was necking. Meanwhile, seven bars of SPPC02 dan SPPC03 were fractured and one was found necking in SPPC03. The locations were ±20-30mm from the pile cap surface. It indicated that the anchorage length of the PC wires was sufficient to prevent the slip of the connection. The amount of reinforcement in the pile cap was also adequate since the concrete spalling only occurred on the concrete cover.

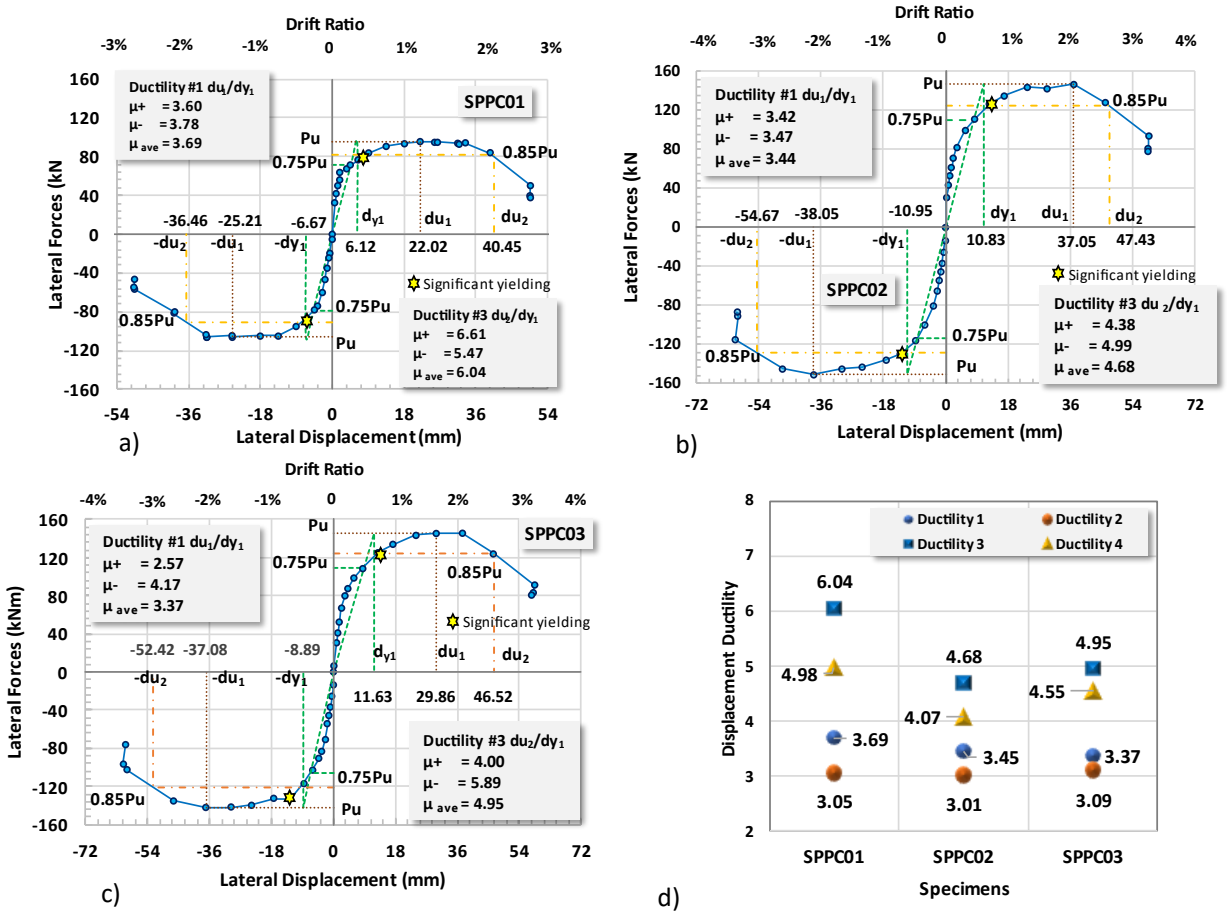

Figure 5 Determination of ductilities: a)SPPC01; b)SPPC02; c)SPPC03 and d) the summary of ductility values

3.3. The Ductility

Displacement ductility is determined as a ratio of ultimate displacement (d_u) to yield displacement (d_y). For reinforced concrete structures, d_y is not well defined due to the nonlinearity of two materials, i.e., concrete and steel. The are two common methods to define yield displacement. Firstly, It is based on an equivalent area of the bilinear elastoplastic curve and it is constructed where the energy absorption is equal (Yang *et al.*, 2020; Guo *et al.*, 2017; Wang *et al.*, 2014). Secondly, the yield line is defined as a secant stiffness at 75% of the ultimate lateral load (Irawan *et al.*, 2017). The latter definition method is more reliable for concrete structures since it considered the reduction of stiffness due to cracking prior to the yielding.

The ultimate deformation has several assumptions. The two most definitions used by a researcher are the displacement corresponding to the peak load (Antonius *et al.*, 2019; Guo *et al.*, 2017; Yang and Wang, 2016) and the post-peak displacement where the load has a small reduction. Different reduction factors were used by the preceding researcher, 15% (Yang *et al.*, 2020), 20% (Zhang *et al.*, 2019), and 30% (Bang *et al.*, 2016). In this study, a 15% strength reduction was chosen since the result was more conservative.

Table 3 Different Values of Ductility

	SPPC01			SPPC02			SPPC03		
	Pull μ-	Push μ+	μavg	Pull μ-	Push μ+	μavg	Pull μ-	Push μ+	μavg
Ductility #1	3.78	3.60	3.69	3.47	3.42	3.45	4.17	2.57	3.37
Ductility #2	3.20	2.90	3.05	2.86	3.15	3.01	3.72	2.46	3.09
Ductility #3	5.47	6.61	6.04	4.99	4.38	4.68	5.89	4.00	4.95
Ductility #4	4.63	5.33	4.98	4.11	4.04	4.07	5.26	3.84	4.55

Two different yield and ultimate displacements that are usually adopted by the former researcher are used and four different ductility values are gained. Table 3 presents the result. The first yield displacement (dy_1) is defined based on secant stiffness whereas the second yield (dy_2) is based on the elastoplastic equivalent curve. Meanwhile, du_1 and du_2 are the displacements corresponding to the peak load and the post-peak load with a reduction of 15%, respectively. The definition of ductility #1 and #3 are described in Figure 5. Ductility #2 and #4 are the ratios of du_2 to dy_1 and dy_2, respectively. The comparison of two different approaches to yield displacement is presented in Table 4. As shown, since dy_2 is slightly higher than dy_1, hence ductility #2 and #4 are lesser.

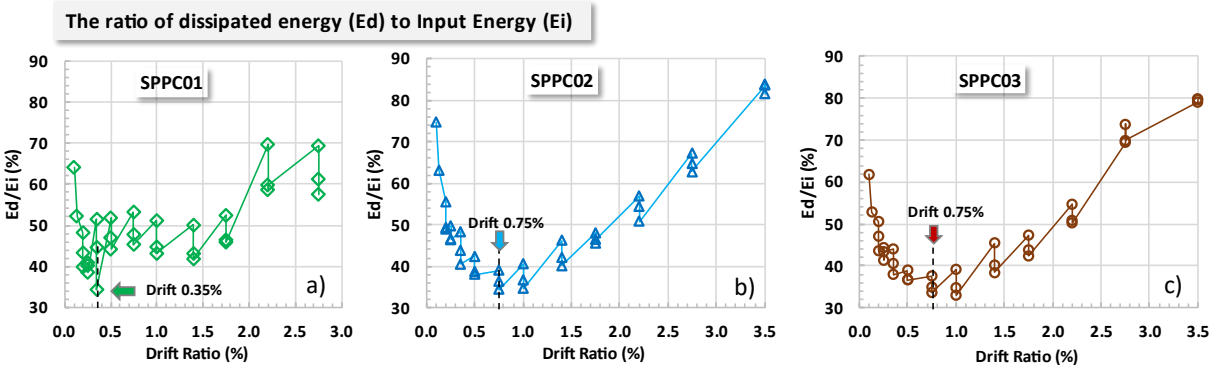

Figure 6 The ratio of dissipated energy (Ed) to input energy (Ei): a)SPPC01, b)SPPC02, c)SPPC03

To confirm the occurrence of yielding, the dissipated energy was observed. It is the energy absorbed by the structure during the inelastic stage which is indicated by the area of the hysteresis curve of each cycle. The input energy is the area below the force-

displacement curve. Figure 6 presents the ratio of the dissipated energy (Ed) to the input energy (Ei). The significant yield is shown as the minimum ratio where the amount of dissipated energy starts to increase rapidly. The data appears scattered for SPPC01 and a drift of 0.35% is the lowest point before it escalated. The significant yield occurred at a drift of 0.75% for SPPC02 and SPPC03. The comparisons of possible occurrences of yielding are presented in Table 4. Dy_1 has a closer value to the significant yield than dy_2 for SPPC01. Meanwhile, dy_2 estimates the occurrence of significant yield better than dy_1 for SPPC02 and SPPC03.

The summary of ductility values based on two different yields and ultimate displacements is presented in Figure 5. The range of ductility values of SPPC01 is relatively large about 3 scales. Meanwhile, SPPC02 and SPPC03 have ductility from 3.01 to 4.95. Referring to the meaning of ductility as the capacity of the structure to deform up to the post-peak stage without significant loss of strength, hence, du_2 is the precise definition. The results are named ductility #3 and #4. The difference in value is lesser from 0.5 to 1 as follows: 4.98 and 6.04 for SPPC01, 4.07 and 4.68 for SPPC02, and 4.55 to 4.95 for SPPC03. Based on significant yielding, ductility #5 was determined and the results were 6.10, 3.78, and 3.66 for SPPC01, SPPC02, and SPPC03, respectively. The values are lower than ductility #3 and #4 for SPPC02 and SPPC03.

Table 4 The comparison of possible yield displacement (dy)

Specimens	dy_1 (mm)		dy_2 (mm)		Significant Yielding (sy) (mm)	Ductility #5 (du_2/sy)
	Push	Pull	Push	Pull		
SPPC01	6.12	-6.67	7.59	-7.88	6.3 (0.35%)	6.10
SPPC02	10.83	-10.95	11.75	-13.30	13.5 (0.75%)	3.78
SPPC03	11.63	-8.89	12.13	-9.96	13.5 (0.75%)	3.66

The displacement ductility of the SPPC01, the spun pile without concrete infill, is higher than other specimens except ductility #1. This was because the yield occurred earlier and the post-peak behavior before the strength drop was longer than other specimens. Meanwhile, the ductility of SPPC02 and SPPC03 is similar referring to ductility #1 and #2. However, the post-peak displacement of SPPC03 is slightly longer than SPPC02 and therefore SPPC03 is more ductile based on ductility #3 and #4.

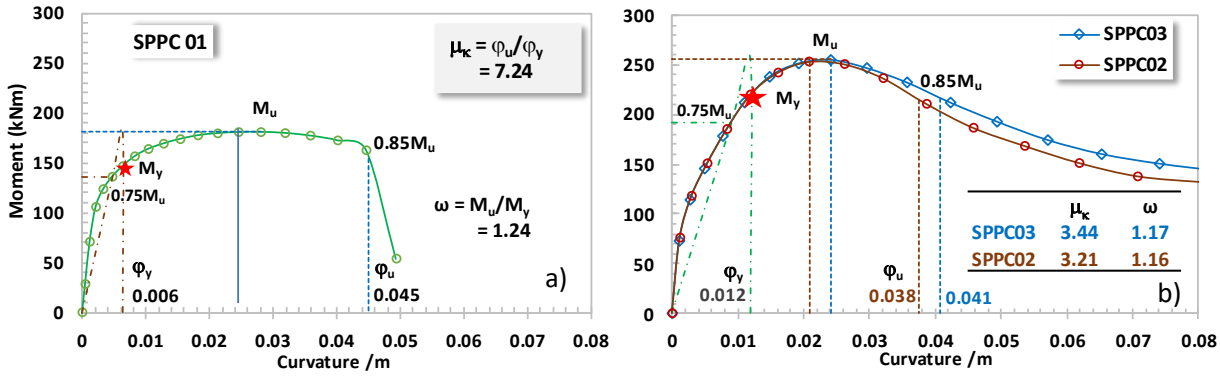

Figure 7 The moment curvature: a) SPPC01 and b) SPPC02/SPPC03

As discussed earlier, displacement ductility (DD) was strongly affected by curvature ductility (CD) and the over-strength ratio (OSR) (Chiou *et al.*, 2011). Analysis of the CD of the specimens is shown in Figure 8. All specimens have a lower CD which was below 10. The moment curvature of SPPC02 and SPPC03 are similar until the maximum moment was reached and then the strength degradation of SPPC03 is more delicate than SPPC02. Therefore, the curvature ductility of SPPC03 is slightly higher than SPPC02. The ductility

that denotes this fact is ductility #3, where the ultimate displacement is at the post-peak load. As shown, SPPC01 has the highest CD and OSR. Therefore, the displacement ductility of this specimen is higher.

SPPC01 seems more ductile than the other specimens. This finding is cross-checked with the dissipated energy since the structure is expected to be ductile to absorb the earthquake energy. The comparison of the cumulative dissipated energy is shown in Figure 8. Poor energy dissipation is noticed on SPPC01 where the cumulative energy dissipation at drift 2.75% is 34% lower than SPPC02.

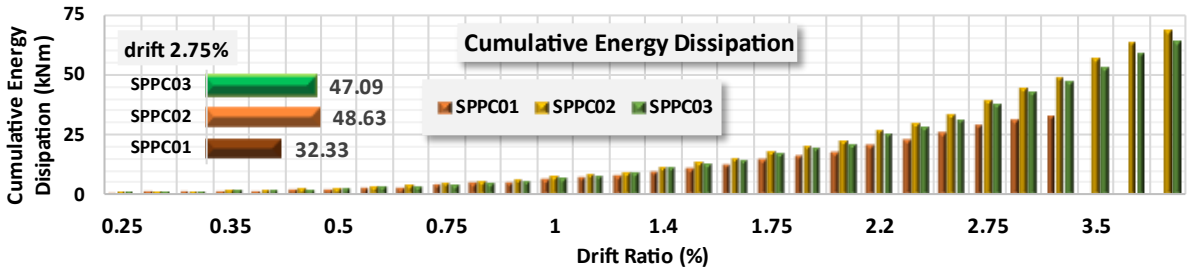

Figure 8 The Cumulative energy dissipation

4. Conclusions

The experimental study showed that the spun pile to pile cap connections behaved as fixed restrained with no slip detected. The failure mode was crushing of the concrete and almost all prestressed wires fractured at the connection region. Flexural crack dominated the crack pattern.

The displacement at post-peak load with the strength reduction of 15% is appropriate to determine ultimate displacement d_u. Meanwhile, the secant stiffness approach is preferred to define yield displacement d_y. Four variation values of ductility were obtained based on two definitions of d_u and d_y. The range values are considered large which are 3.05 to 6.04 for SPPC01, 3.09 to 4.95 for SPPC02, and 3.01 to 4.68 for SPPC03. All specimens could reach the ductility limit, of three, referring to ATC 96 and JRA 2002. Hence, the low confinement spun pile showed adequate performance.

SPPC01, the empty spun pile, showed poor energy dissipation than SPPC02 and SPPC03 which reveals from the cumulative dissipated energy and the wider crack distribution on the spun pile. Non-shrinkage concrete strength affects the post-peak behavior of SPPC03 where its strength drops more faintly than SPPC02. It has slightly better displacement ductility when post-peak is defined as the maximum displacement.

Acknowledgments

The research was supported by the Indonesia Ministry of Research and Universitas Indonesia through Applied Research, contract number NKB-254/UN2.RST/ HKP.05.00/2021 and PT Wijaya Karya Beton, Tbk.

References

ACI Committee, 2019. ACI 318-19: Building Code Requirements for Structural Concrete and Commentary. American Concrete Institute: Farmington Hills, MI, USA

AASHTO, 2011. *AASHTO Guide Specifications for LRFD Seismic Bridge Design*. AASHTO. 2nd ed

Antonius., P., Harprastanti, P., 2019. Experimental Study of the Flexural Strength and Ductility of Post Burned Steel Fiber RC Beams. *International Journal of Technology*, Volume 10(2), pp. 428–437

Bang, J.W., Oh, S.J., Lee, S.S., Kim, Y.Y., 2016. Pile-cap Connection Behavior Dependent on the Connecting Method between PHC pile and Footing. *Journal of the Korea Institute for Structural Maintenance and Inspection*, Volume 20(3), pp. 25–32

Budek, A., Benzoni, G., 2009. Obtaining Ductile Performance from Precast, Prestressed Concrete Piles. *PCI Journal*, Volume 54(3), pp. 64–80

Budek-Schmeisser, A., Benzoni, G., 2008. Rational Seismic Design of Precast, Prestressed Concrete Piles. *PCI Journal*, Volume 53(5), pp. 40–53

Chai, Y.H., Hutchinson, T.C., 2002. Flexural Strength and Ductility of Extended Pile-Shafts. II: Experimental Study. *Journal of Structural Engineering*, Volume 128(5), pp. 595–602

Chiou, J.S., Tsai, Y.C., Chen, C.H., 2011. Simple Estimation for Ductility Capacity of a Fixedhead Pile in Cohesive Soils. *Canadian Geotechnical Journal*, Volume 48(10), pp. 1449–1460

Fanous, A., Sritharan, S., Suleiman, M., Huang, J.W., Arulmoli, A.K., 2010. Minimum Spiral Reinforcement Requirements and Lateral Displacement Limits for Prestressed Concrete Piles in High Seismic Regions. *Reports and White Papers*, pp. 1–164

FEMA P-750, 2009. *NEHRP Recommended Seismic Provisions*. Federal Emergency Management Agency

Guo, Z., He, W., Bai, X., Chen, Y.F., 2017. Seismic Performance of Pile-Cap Connections of Prestressed High-Strength Concrete Pile with Different Details. *Structural Engineering International*, Volume 27(4), pp. 546–557

Irawan, C., Djamaluddin, R., Raka, I.G.P., Suprobo, P., 2018. Confinement Behavior of Spun Pile Using Low Amount of Spiral Reinforcement - An Experimental Study. *International Journal on Advanced Science, Engineering and Information Technology*, Volume 8(2), pp. 501–507

Irawan, C., Raka, I.G.P., Djamaluddin, R., Suprobo, P., 2017. Ductility and SEismic Performance od Spun Pile Under Constant Axial and Reverse Flexural Loading. *International Symposium on Concrete Technology (ISCT 2017)*, pp. 35–44

Ling, J.H., Lim, Y.T., Jusli, E., 2023. Methods to Determine Ductility of Structural Members: A Review. Journal of the Civil Engineering Forum, Volume 9(2), pp. 181–194

Pramono, S., Prakoso, W.A., Rohadi, S., Karnawati, D., Permana, D., Prayitno, B.S., Rudyanto, A., Sadly, M., Sakti, A.P., Octantyo, A.P., 2020. Investigation of Ground Motion and Local Site Characteristics of the 2018 Lombok Earthquake Sequence. *International Journal of Technology*. Volume 11(4), pp. 743–753

Wang, T., Yang, Z., Zhao, H., Wang, W., 2014. Seismic Performance of Prestressed High Strength Concrete Pile to Pile Cap Connections. *Advances in Structural Engineering*, Volume 17(9), pp. 1329–1342

Yang, Z., Li, G., Nan, B., 2020. Study on Seismic Performance of Improved High-Strength Concrete Pipe-Pile Cap Connection. *Advances in Materials Science and Engineering*, Volume 2020, pp. 1–22

Yang, Z., Wang, W., 2016. Experimental and Numerical Investigation on The Behaviour of Prestressed High Strength Concrete Pile-to-Pile Cap Connections. *KSCE Journal of Civil Engineering*, Volume 20(5), 1903–1912

Zhang, X., Niu, S., Yan, J.B., Zhang, S., 2019. Seismic Behaviour of Prestressed High-Strength Concrete Piles Under Combined Axial Compression and Cyclic Horizontal Loads. *Advances in Structural Engineering*, Volume 22(5), pp. 1089–1105